

PAPER • OPEN ACCESS

A biomimicking design for mechanical knee joints

To cite this article: Felix Russell *et al* 2018 *Bioinspir. Biomim.* **13** 056012

View the [article online](#) for updates and enhancements.

You may also like

- [An innovative MRE absorber with double natural frequencies for wide frequency bandwidth vibration absorption](#)
Shuaishuai Sun, Jian Yang, Weihua Li et al.
- [Finding the density of a liquid using a metre rule](#)
K N Chattopadhyay
- [Chordwise implementation of pneumatic artificial muscles to actuate a trailing edge flap](#)
R D Vocke, C S Kothera and N M Wereley

Bioinspiration & Biomimetics

OPEN ACCESS



CrossMark

PAPER

A biomimicking design for mechanical knee joints

RECEIVED

19 January 2018

REVISED

26 June 2018

ACCEPTED FOR PUBLICATION

16 July 2018

PUBLISHED

2 August 2018

Original content from this work may be used under the terms of the [Creative Commons Attribution 3.0 licence](#).

Any further distribution of this work must maintain attribution to the author(s) and the title of the work, journal citation and DOI.



Felix Russell^{1,5}, Yipeng Zhu², William Hey¹, Ravi Vaidyanathan¹ and Peter Ellison^{1,3,4}

¹ Mechanical Engineering Department, Imperial College London, London, United Kingdom

² Faculty of Engineering, Zhejiang University, 38 Zheda Road, Hangzhou, People's Republic of China

³ Department of Clinical Medicine, University of Bergen, Bergen, Norway

⁴ Department of Orthopaedic Surgery, Haukeland University Hospital, Bergen, Norway

⁵ Author to whom any correspondence should be addressed.

E-mail: felix.russell12@imperial.ac.uk, pheo@zju.edu.cn, william.hey15@imperial.ac.uk, r.vaidyanathan@imperial.ac.uk and peter.ellison@outlook.com

Keywords: biomimetics, biomechanics, robotics, ligaments, above knee prostheses, condylar knee, lower limb

Abstract

In this paper we present a new bioinspired bicondylar knee joint that requires a smaller actuator size when compared to a constant moment arm joint. Unlike existing prosthetic joints, the proposed mechanism replicates the elastic, rolling and sliding elements of the human knee. As a result, the moment arm that the actuators can impart on the joint changes as function of the angle, producing the equivalent of a variable transmission. By employing a similar moment arm—angle profile as the human knee the peak actuator force for stair ascent can be reduced by 12% compared to a constant moment arm joint addressing critical impediments in weight and power for robotics limbs. Additionally, the knee employs mechanical ‘ligaments’ containing stretch sensors to replicate the neurosensory and compliant elements of the joint. We demonstrate experimentally how the ligament stretch can be used to estimate joint angle, therefore overcoming the difficulty of sensing position in a bicondylar joint.

1. Introduction

Walking on flat ground is more energy efficient in humans and other legged animals than in current robotic walking mechanisms [1]. However, those robots that do achieve similar levels of efficiency, such as the Cornell Ranger [2], are often incapable of performing high load tasks. The mechanism and control strategy of the human leg, however, exhibits both efficiency for lower load tasks as well as capacity for high load activities such as stair ascent. It is therefore unsurprising that considerable research effort has already gone into replicating human properties in mechanical joints [3].

For walking robots this has taken the form of tendon-like cables which are used to reduce energy consumption by removing actuator mass from the legs themselves so that they can be located nearer the robot centre of mass, in the main body [1]. Additionally, reductions are achieved by adding springs to the joints or actuators to help replicate human dynamics [2, 4, 5]. Martinez-Villalpando *et al* and Geeroms *et al* [6, 7] apply a similar approach to a prosthetic knee. Springs are added to the joint in series or parallel with the actuation and the result is a reduction in energy consumption for level gait [8].

These studies, however, take a more abstract biomimicking approach than the work presented here. The efficiency of human gait is likely to stem from multiple aspects of the system, including: control strategy, joint design and actuation. With this in mind, this paper focusses on the sensory-mechanical aspect as a first step with the intention of adding human-like control and actuation strategies in future work. Robotic simulations have shown that a joint motion that more closely matches that of the human knee can reduce energy consumption for gait [9]. In this paper human knee features such as a varying moment arm, rolling condyles and elastic ligaments are incorporated into a joint design.

This work seeks to show that it is possible to design a bioinspired knee with improved mechanical performance compared to a constant moment arm knee in order to address weight and power limitations in the current generation of lower limb robotic systems. This is to be achieved via a cable driven bicondylar joint with a variable moment arm similar to the biological knee. A comparison will be made between the minimum actuator size required for a high load task, a stair ascent, for both the bicondylar knee and a system with a constant moment arm.

Additionally, the moving centre of rotation makes fitting an encoder onto a joint of this type difficult.

Inspired by the human knee a sensor has been designed that uses the stretch of elastic mechanical ‘ligaments’ in a bicondylar joint in order to estimate joint angle. As well as source information on joint state these provide a form of adjustable parallel compliance.

1.1. Current prosthetic joint designs

Commercially available passive and negative net power above knee prostheses already use variable moment arms as part of their designs. This is done by utilising four bar mechanisms [10–12] with bar layouts selected for both stance stability and ease of swing extension. Additionally, these designs often employ compliant elements for extension assist or to absorb energy when going down inclines.

Positive power prostheses such as the ÖSSUR power knee [13] are already commercially available but do not make use of variable moment arms. They are heavy, with a mass of 3.9 kg [13], 33% more than the average human shank [14]. However there are known benefits to these products. Symmetry is improved when compared to a microprocessor knee [15] and the power available for sit to stand tasks [16] and stair ascent [17] is increased. Nevertheless, they are not currently fully able to restore function, demonstrated by the intact limb often carrying more of the load than the leg fitted with the prosthesis [16, 17]. This suggests that the compensation provided by the powered knee is not yet adequate and an increase in available joint torque without an increase in weight would benefit users.

1.2. The human knee

The overall structure of the human knee is that of two smooth condyles at the end of the femur and tibia that roll and slide over each other throughout joint motion. These surfaces are held together by ligaments and other soft tissues to resist movement of the joint outside of the normal range [18]. The four ligaments are elastic [19], ensuring that the condyles are always in contact. As a result the centre of rotation in the sagittal plane moves relative to both bones as they rotate [20]. A further consequence is that the ligaments stretch varies during joint motion [21]. These ligaments also contain mechanoreceptors that signal this stretch [22, 23] for use in joint control [24, 25].

The knee is driven in the extension direction by the quadriceps muscles via tendons and a patella. The patella runs against the smooth surface of the femoral condyle. It is attached at the femoral end to the quadriceps via the quadriceps tendon and at the tibial end to the tibia via the patella tendon. This tendon driven actuation, combined with the moving centre of rotation, produces a moment arm of the quadriceps that changes as a function of angle [20, 26]. This leads to a type of variable mechanical advantage or ‘gearing’. Where the moment arm is small the amount of muscle displacement required for a change in angle is reduced but the joint moment per unit force is lower. Where the

moment arm is large finer control and higher forces are possible but a larger muscle displacement is necessary.

1.3. Work to date

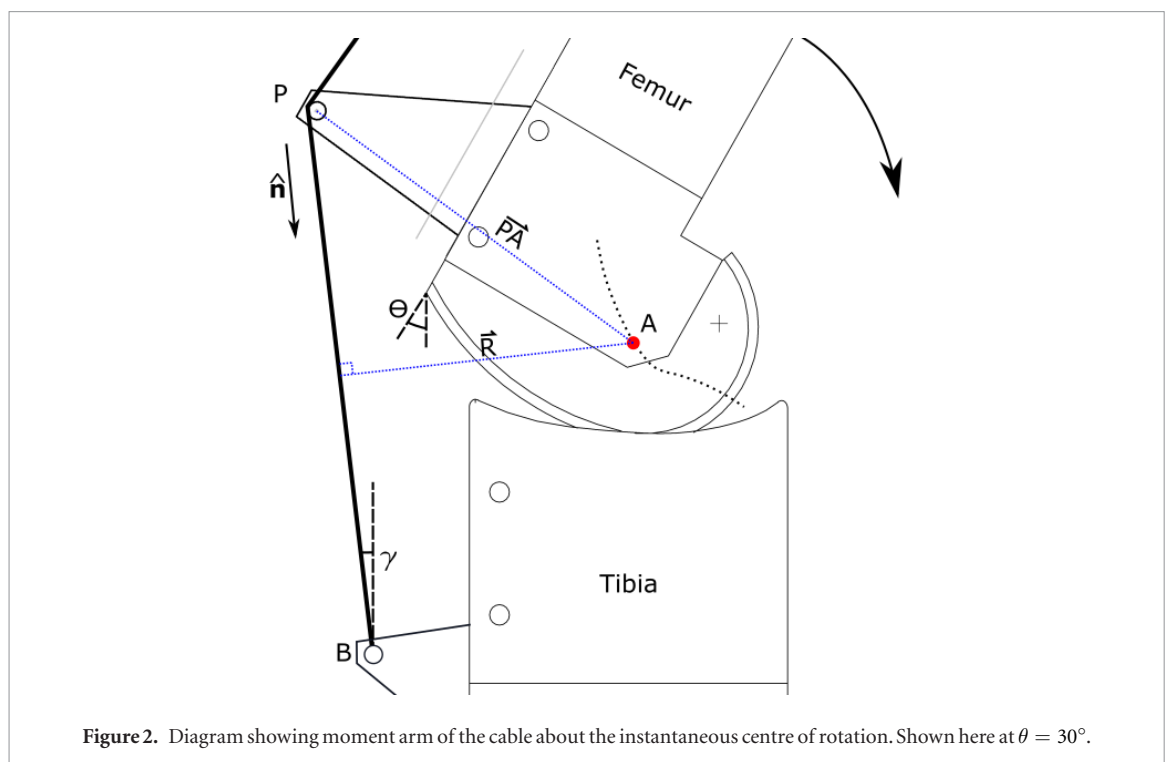
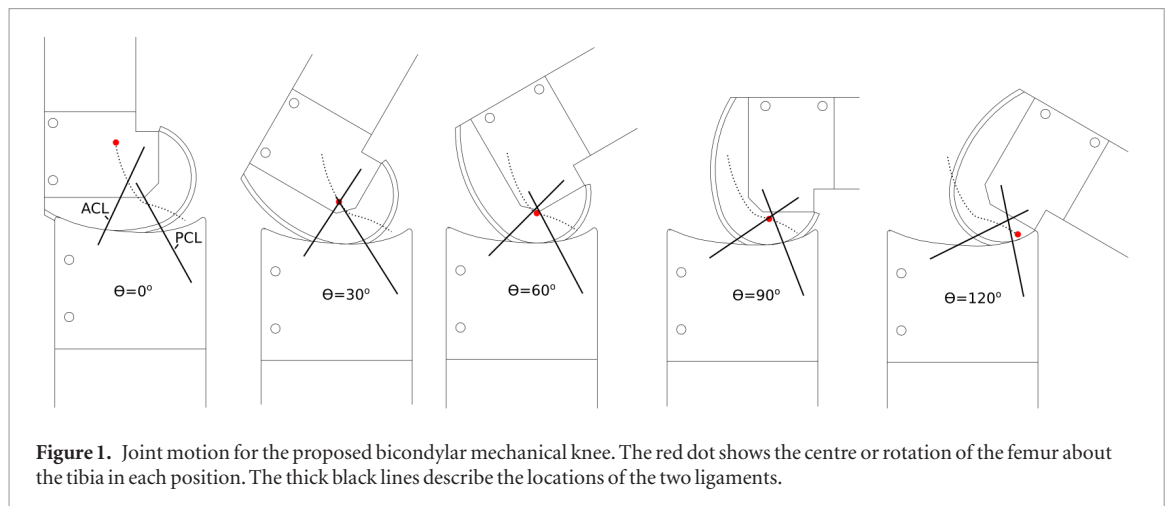
Previous studies that investigate the replication of the human knee have used simpler methods than the one presented here. These range from use of a pin joint and cam [27, 28] to those that use four bar mechanisms to achieve the desired motion [29, 30]. Each of these papers succeeds in capturing particular aspects of knee joint performance with regards to kinematics, stiffness or moment arm. However we believe that by looking at the physical and sensory make-up of the human knee in detail, it will be possible to capture all these features, and more, in a single joint design. One research group that has already begun this investigation is that of Etoundi *et al* [31, 32] who have built a condylar knee design without tendons or compliance and found it to have mechanical benefits. The design presented here goes further by including elastic stretch sensing ligaments and a biologically derived condyle shape. In our previous work [33] a design for stretch sensing compliant ligaments and a condylar knee was presented. Using this first iteration of the joint we show that stretch in these ligaments is a function of joint forces and angular velocity as well as joint position.

1.4. Aims of this work

In this paper the concept is taken further in two ways: Firstly an optimisation is performed on the proposed second iteration of the joint in order to tune the design to more closely mimic the human moment arm curve. We then see the effect this might have on the actuator sizes required for a high load task. Secondly, the version of the joint that was presented in Russell *et al* [33] is incorporated into a newly built squatting rig in order to develop and test a method of estimating joint angle using ligament stretch. It is hypothesised that the fusion of improved mechanical design and control feedback based on estimated joint angle will provide a foundation for a new range of lighter and more controllable robot legs.

We seek to assess:

- (i) *Patella position tuning (section 2.1)*: whether replicating the human knee moment arm - angle relationship in a biomimicking cable driven joint can be achieved by optimising the cable attachment points. This optimisation is performed on a computer model of the joint (figures 1 and 2) where the difference compared to the human value is minimised (figure 3). The potential benefits of this design with regards to actuator size are assessed.
- (ii) *Ligament stretch for joint position estimation (section 2.2)*: whether stretch information from the compliant ligaments in the joint



can provide angle information. Testing is to be done using the same first iteration of the joint from Russell *et al* [33] but with a squatting rig so that the joint experiences more realistic loads. Tests are performed to assess angle estimation accuracy as well as whether this estimate can be used to control the joint without any other sensing.

2. Methods

Our joint has a particular geometry chosen such that compliant ligaments within the joint stretch in a way that matches measurements from humans [21]. The design has the following human-like features:

- Two bio-derived joint condyles that can slide over each other and take the compressive load required of the joint.

- Two cruciate ligament analogues that are both elastic and have stretch sensing capability.
- Cable driven actuation to simulate the tendons and a mechanical analogue of the patella.
- A centre of rotation that changes position as a function of the joint angle.

The joint designs used in sections 2.1 and 2.2 differ. The joint that has been built for position estimation using ligament stretch (section 2.2) is the first iteration of the bicondylar joint. This design was first presented in Russell *et al* [33]. The joint used in the computer model (section 2.1) is a second iteration of the joint design that has been manufactured but not tested. Details of both the these designs are presented under sections 2.1.1 and 2.2.1.

Perry [34] showed that during gait sagittal plane movements dominate compared to transversal and frontal knee movements. Thus for both these designs these extra movement directions have been omitted.

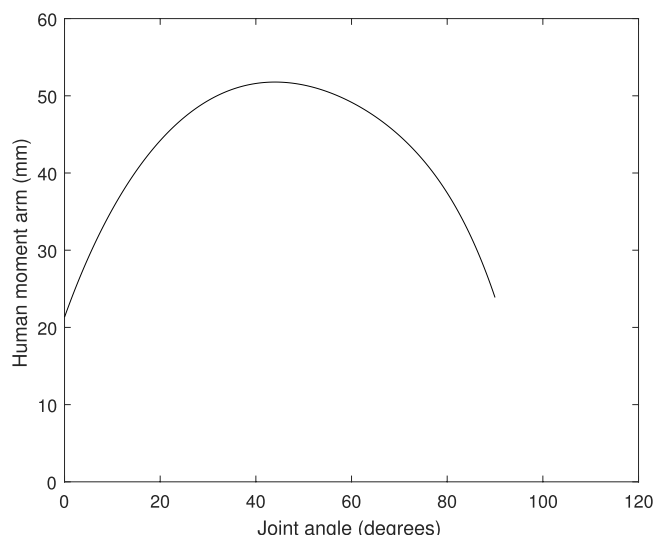


Figure 3. Moment arm of the human knee as a function of joint angle. Taken from Krevolin [26] using the average of male and female datasets and performing a 4th order polynomial fit.

2.1. (i) Patella position tuning

To represent the patella more simply than the floating bearing present in the human knee two designs were investigated: one in which the patella was represented as a pulley attached to the femur (figure 4(a)) and one in which it was represented as a bracket attached to the tibia (figure 4(b)). The method detailed here allowed us to decide which of these representations was the closer match to the human joint in terms of moment arm profile.

In addition, for each geometry, a further scenario was simulated where the centre of rotation was fixed at the coordinate system origins marked in figure 4. This allowed us to see what additional benefit the moving centre of rotation provided compared to a tendon driven but fixed centre of rotation knee.

Both layouts were optimized so that the moment arm as closely as possible matched the moment arm of the human knee. The two layouts were then compared to see which produced the better fit. In both cases the cable tension was controlled by actuators that simulated the quadriceps i.e. attached to the femur.

2.1.1. Selection of joint geometries

The latest version of the design is used in the optimisation presented in this section. It has ligament attachment points and condyle shapes chosen based on data from cadaver studies. The femoral condyle has been taken from a sagittal plane section of the bone scan from Isaza *et al* [35]. The ligament attachment points are based off locations shown in Fuss' [36] paper on ligament attachment points; ligament lengths were taken from ACL data from Cohen *et al* [37] and PCL values were found by taking measurements from the drawings in Fuss [36] scaled using the Cohen ACL value. The relationship between ligament stretch and joint angle was taken from a weighted average of the ligament bundle measurements in Kurosawa *et al* [21]. A tibia profile was then designed such that there is no

intersection of the two condyles as the joint rotates but a point of contact is maintained at all times. The resulting ligament positions and condyle shapes are shown in figure 1.

2.1.2. Calculation of extension moment arm

As the femur rotates relative to the tibia all parts fixed to the femur rotate with it. The moment arm acting on the femur about its centre of rotation can be found by equation (1) where point P is the femur fixed patella or tendon attachment point, point A is the instantaneous centre of rotation of the femur about the tibia (figure 1) and \hat{n} is the unit vector of the force that is acting to rotate the femur (figure 2)

$$R = |\vec{PA} - ((\vec{PA} \cdot \hat{n})\hat{n})|. \quad (1)$$

The centre of rotation was used for moment calculations because the normal contact force from the condyles has to pass through this point in order for the surfaces to remain non-intersecting. The ligament forces, which are small in magnitude compared to the contact or tendon forces, are known to pass close to this point and so will only be able to impart a small moment in comparison with that imparted by the cable. This is similar to methods used by Smidt [20] and Krevolin [26] to measure knee moment arms in cadavers.

For any particular cable arrangement the moment arm relationship calculated by the method above was compared to the human moment arm, r_{θ} , from Krevolin *et al* [26] (figure 3). The sum of absolute differences between the two was calculated to measure the degree of similarity between the two.

2.1.3. Constraints

Boundary conditions were chosen to limit the size of the joint mechanism and to maintain a broadly human-like geometry. The patella and tendon attachment positions were limited, as shown in figure 4.

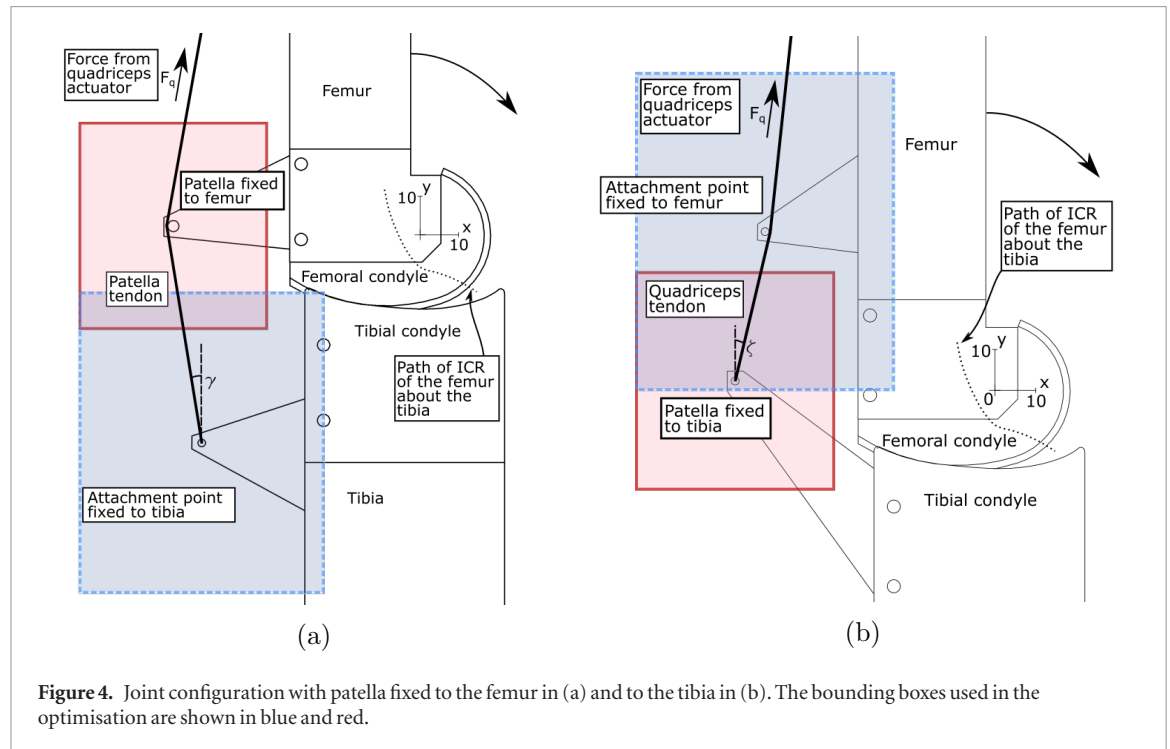


Figure 4. Joint configuration with patella fixed to the femur in (a) and to the tibia in (b). The bounding boxes used in the optimisation are shown in blue and red.

To ensure that the cable forces would act more or less the same directions as in the human knee the angles γ and ζ at a joint angle of 0° were constrained. Van Eijden *et al* [38] show that, in humans, the angles between the patella and quadriceps tendons and the axis of the femur are 20° and 10° degrees respectively at a joint angle of 0° . Thus the values in equations (2) and (3), 20° either side of Van Eijden's values, were selected. This will reduce the chance of large shear forces across the joint, which could induce unstable sliding between the condyles.

$$0^\circ \leq \gamma_{\theta=0} \leq 40^\circ \quad (2)$$

$$-10^\circ \leq \zeta_{\theta=0} \leq 30^\circ. \quad (3)$$

2.1.4. Optimisation procedure

The optimisation of the four variables that describe the x and y positions of both the tendon attachment points and patella location was carried out first by genetic algorithm (population = 100, generations = 200, crossover fraction = 0.3) using the Matlab genetic algorithm toolbox. The nonlinear constraint on γ and ζ was enforced using a penalty method. To meet the requirements for biomimetic optimisation suggested by Haberland *et al* [39] each optimisation was run 20 times with different random starting populations in order to reduce the chance of optimising to a local minimum. This means that a total of 20000 starting configurations were evaluated within the 4D possibility space. Increasing the number of times the algorithm was run beyond this point revealed no new minima. The optimal result from the genetic algorithm was then used as the initial point for the standard Matlab interior point minimiser to further improve the precision of optimisation.

2.1.5. Required actuator size

The calculations for a common high load task, a stair ascent, were performed for each optimized design and compared to a constant moment arm joint with the same actuator stroke length:

The total actuator stroke length, ' L_{stroke} ', required for the full 120° of joint motion was found as the difference between the distance \overrightarrow{PB} (figure 2) at 0° and at 120° . A constant moment arm joint that used an actuator of the same length would have to have a moment arm of R_{const} (equation (4)).

$$R_{const} = \frac{L_{stroke}}{\theta_{range}}. \quad (4)$$

Costigan *et al* [40] show that the maximum knee moment per unit body weight required for this activity is $\max(M_\theta) = 1.1 \text{ Nm}(\text{kg})^{-1}$ which, using a joint with constant moment arm of size R_{const} , would require a maximum actuator force $\max(F_{const})$:

$$\max(F_{const}) = \frac{\max(M_\theta)}{R_{const}}. \quad (5)$$

Similarly for the bicondylar joint design the actuator force at every angle can be found using the external knee moment curve M_θ from Consigan *et al* [40] and the moment arm curve of our joint R_θ (figure 8(a)). The required actuator force as a function of angle can be found by equation (6).

$$F_\theta = \frac{M_\theta}{R_\theta}. \quad (6)$$

$\max(F_{const})$ and the maximum value of F_θ can be compared. A smaller $\max(F_\theta)$ compared to $\max(F_{const})$ means that the peak force required for the stair climb task is smaller with the bicondylar joint. These forces are proportional to the minimum area of

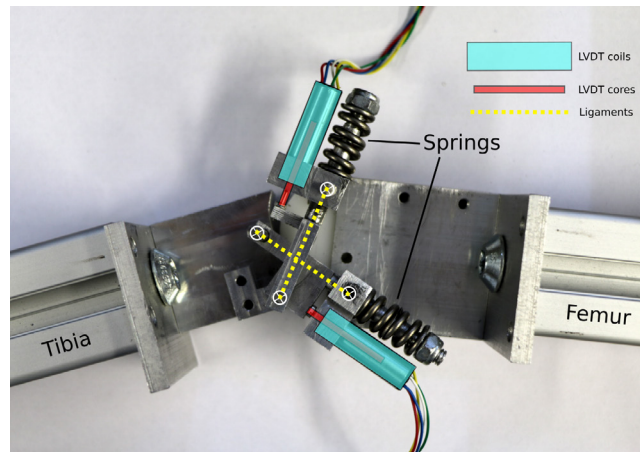


Figure 5. Cross-section of the joint showing the ligaments in the first iteration of the joint design that was used in section 2.2. The LVDT core and coils can slide with respect to each other. The signal from the coils can then be conditioned to give a DC signal proportion to the core position and, therefore, ligament length.

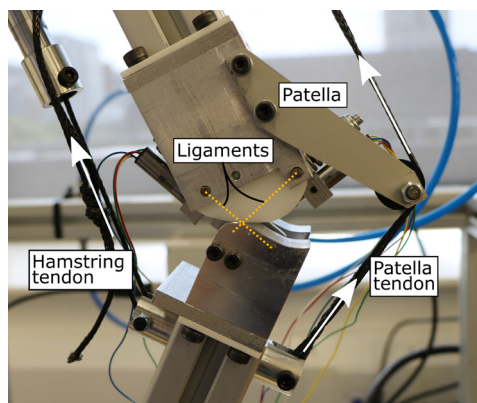


Figure 6. First iteration of the knee joint with elastic stretch sensing ligaments.

a pneumatic or hydraulic cylinder required to drive the joint. Since the lengths of the cylinders in both scenarios are the same the maximum force can also be used as a measure of the required cylinder volume.

2.2. (ii) Ligament stretch for joint position estimation

Estimation of joint position using ligament stretch was performed on a earlier version of the joint [33] than that described in section 2.1. A purpose build squatting rig was built and a condylar joint was manufactured that contained linear variable differential transformers (LVDTs) to measure stretch within elastic mechanical ‘ligaments’ (figures 5 and 6).

2.2.1. Design of the robotic model

The joint itself is the same design as that presented in Russell *et al* [33]. Stretch sensing ligaments were manufactured from aluminium to represent the ACL and PCL within the joint. A series spring provides compliance and a parallel LVDT measures stretch. Figure 5 shows how these ligaments are integrated into the overall joint design. This early version of the

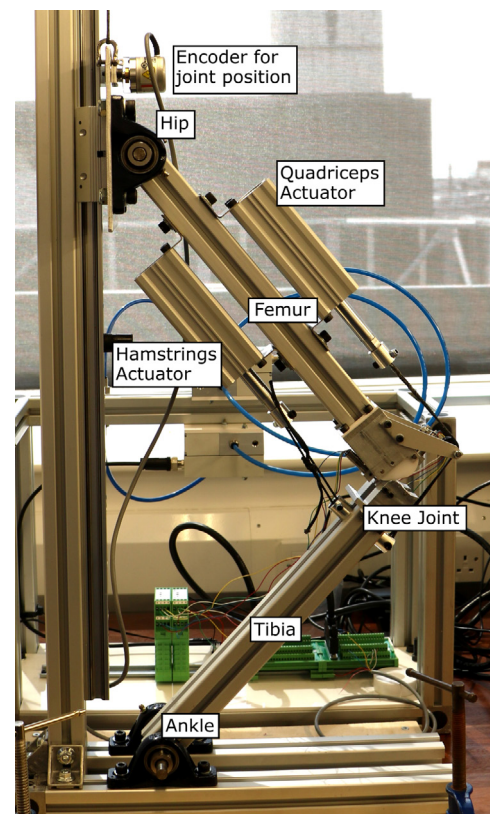
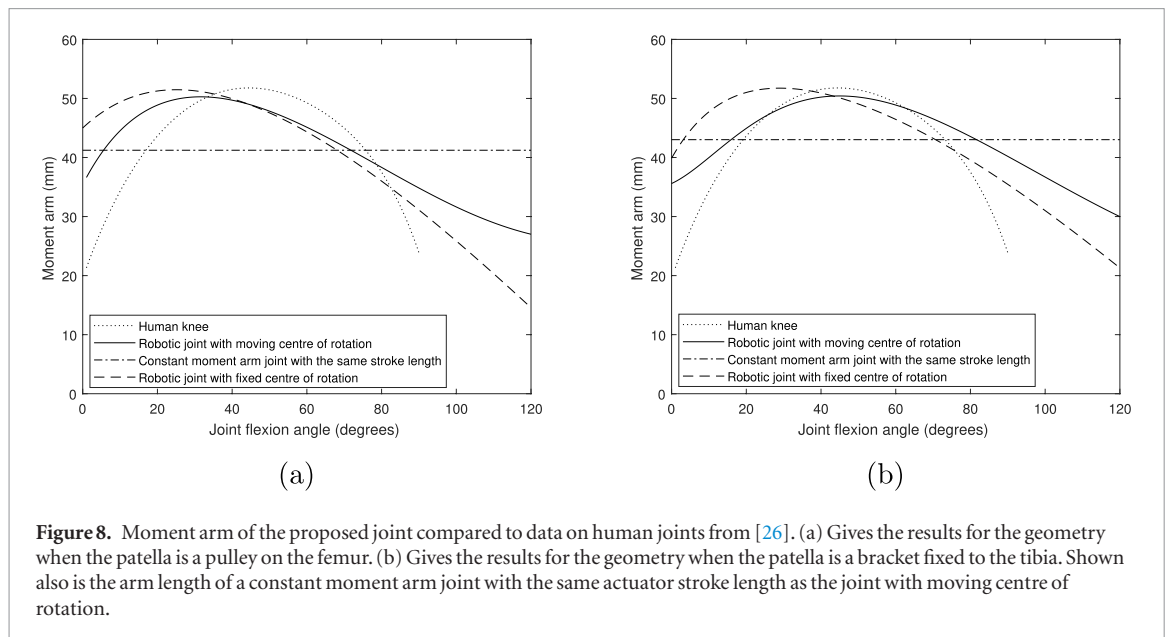


Figure 7. Single leg squat test set up.

joint is designed as a proof of concept for ligament based sensing and the joint geometries do not match the human knee as closely as the design proposed in section 2.1. The ligament attachment positions were chosen so that they were crossed throughout joint motion with the femoral condyle moving anteriorly as joint angle increased; The femoral condyle shape was selected to match the overall proportions, but not shape, of the human knee; The tibial condyle was selected so that at each angle of rotation both a section of the tibial surface is tangential to the



femoral condyle and there is no interference between the surfaces. The joint surfaces are made from acetal and aluminium for the femoral and tibial condyles, respectively. The ligament stiffnesses and lengths have been selected to be in the same range as in the human knee [19, 37].

To simulate a single leg squat (figure 7) a sled and bearing at the hip allowed the proximal end of the femur both vertical translation and sagittal plane rotational degrees of freedom. The distal end of the tibia was fixed to a bearing at the base to represent a fixed foot.

An encoder at the hip was used to provide the measurements of knee joint angle for the training of the estimator and in order to measure the estimator's performance. Before testing began an optical tracking camera was used to find the relationship between the height of the hip measured with the encoder and joint angle. This provided the measurement of the actual joint angle necessary for the training and testing procedures described in section 2.2.2. The muscles were simulated using pneumatic actuators fed by an air supply whose pressure could be controlled digitally.

To control the joint using both actuators a preload was applied to both the quadriceps and hamstrings actuators that was found to be just sufficient to hold the joint at a constant angle. A PID controller then added additional force to either the hamstring or quadriceps depending on whether the joint was required to accelerate in the flexion or extension directions.

2.2.2. Training routine

Ligament stretch as a function of angle was recorded for three types of movement:

- Joint angle linearly increasing over the full range
- Joint angle linearly decreasing over the full range
- Joint angle following a sinusoidal path, extending then flexing

For each task a Levenberg–Marquardt back propagation neural network with 10 perceptrons in the hidden layer was trained with the stretch from both ligaments and the filtered PID output as inputs and joint position as output. The filtered PID output was included in the input to the estimator because previous work [33] has showed that ligament stretch changes as a function of joint forces as well as angle. Since the PID output was proportional to the force from the agonist actuator this gave the estimator extra information that made the joint angle estimate more accurate. Data was collected as the rig performed ramp tests at rates ranging from $2\text{--}21.5\text{ deg s}^{-1}$. The neural network was then trained offline.

The system performance was evaluated in two ways:

- In order to assess the performance of the estimator the estimated joint angle was compared to the known joint angle from the encoder at the hip. This angle was also used as the feedback for the PID controller during these experiments.
- In order to test the usefulness of this estimation the output of the estimator was then used as the position feedback for the PID controller. The quality of this control was compared to the quality of control from the first test when the hip encoder was used.

3. Results

3.1. (i) Patella position tuning

The optimisation was performed on both joint geometries with and without a moving centre of rotation. Figure 8(a) shows the moment arm for the optimum configurations when the patella is represented as a pulley attached to the femur as in figure 4(a). Figure 8(b) shows the moment arm

Table 1. Summary data for figures 8(a) and (b). For each joint configuration the location and magnitude of the maximum moment arm is given alongside two measures of the difference when compared to the moment arm of the human knee.

Joint configuration	Figure	Mean absolute diff. (mm)	Max. absolute diff. (mm)	Angle of max. moment arm ($^{\circ}$)	Max. moment arm (mm)
Patella on femur. Moving COR	8(a)	4.60	15.3	30.7	50.3
Patella on femur. Fixed COR	8(a)	5.84	23.7	25.0	51.4
Patella on tibia. Moving COR	8(b)	3.36	16.3	44.8	50.4
Patella on tibia. Fixed COR	8(b)	4.95	18.6	28.9	51.7
Constant moment arm joint	8(a)	7.53	19.9	—	41.3
Constant moment arm joint	8(b)	7.08	21.7	—	43.0
Human moment arm from [26]	—	—	—	43.9	51.8

Table 2. Total stroke length for each configuration, maximum joint force for stair ascent and the maximum force in a constant moment arm joint with the same stroke length.

Joint configuration	Actuator stroke length (mm)	$\max(F_{\theta})$ (N kg^{-1})	$\max(F_{\text{const}})$ (N kg^{-1})	% force change (%)
Patella on femur. Moving COR	86.4	24.4	26.7	−8.6
Patella on femur. Fixed COR	83.5	24.7	27.6	−10.5
Patella on tibia. Moving COR	90.1	22.5	25.6	−12.1
Patella on tibia. Fixed COR	83.0	23.6	26.2	−9.9

for the optimum configuration when the patella is represented as a bracket attached to the tibia as in figure 4(b). In addition, table 1 shows the performance of the constant moment arm joint as calculated by equation (4) for the moving centre of rotation configurations.

Mean absolute difference, angle of maximum moment arm and value of the maximum moment arm is provided in table 1 for all geometries. The best average fit is achieved with the patella attached to the tibia with moving centre of rotation. In this configuration the mean absolute difference between the bicondylar joint moment arm and the human moment arm between 0° and 90° was 3.36 mm with a maximum difference of 16.3 mm at 90° . The smallest maximum difference was with patella represented as a femur attached pulley although for this configuration the mean difference was larger and location of the maximum moment arm was further from that found in the human knee. For both configurations fixing the centre of rotation makes the fit to the human moment arm poorer than when a bicondylar moving centre of rotation is used. This is the case across all the metrics shown in table 1. In addition, in all cases the constant moment arm joint with the same stroke length as the bicondylar joint showed greater mean and maximum differences than in the equivalent tendon driven configurations.

3.1.1. Required actuator size

The calculations described in section 2.1.5 were performed on each of the four scenarios. The results are presented in table 2. The force reduction for stair climb compared to a constant moment arm joint is

between 8.6% and 12.1% depending on which of the four configurations is chosen.

3.2. (ii) Ligament stretch for joint position estimation

Figure 9 presents the accuracy of the joint position estimate performed offline compared to the position of the joint when measured with an encoder at the hip. The performance of the estimator and controller is given as a mean squared error in table 3. For all tests the controller error was lower in the extension direction than the flexion direction. Joint angle estimation is accurate to better than 1.3° on average for the sinusoid test.

Figure 10 and accompanying table 4 present the performance when using the estimate of joint position using ligament stretch as feedback to the PID controller. The control error in all three test types is higher and has larger standard deviations than when the encoder is used for angle feedback (table 3).

4. Discussion

4.1. (i) Patella position tuning

Using the process described in this paper it is possible to design a joint with a similar relationship between moment arm and angle as in the human knee. This can be achieved by representing the patella as either a smooth pulley on the femur or rigid bracket on the tibia. The configuration with lowest mean difference to the human moment arm was that where the patella was fixed to the tibia and the joint is bicondylar with a moving centre of rotation. Here the maximum moment arm is 50.42 mm achieved at 44.8° , compared

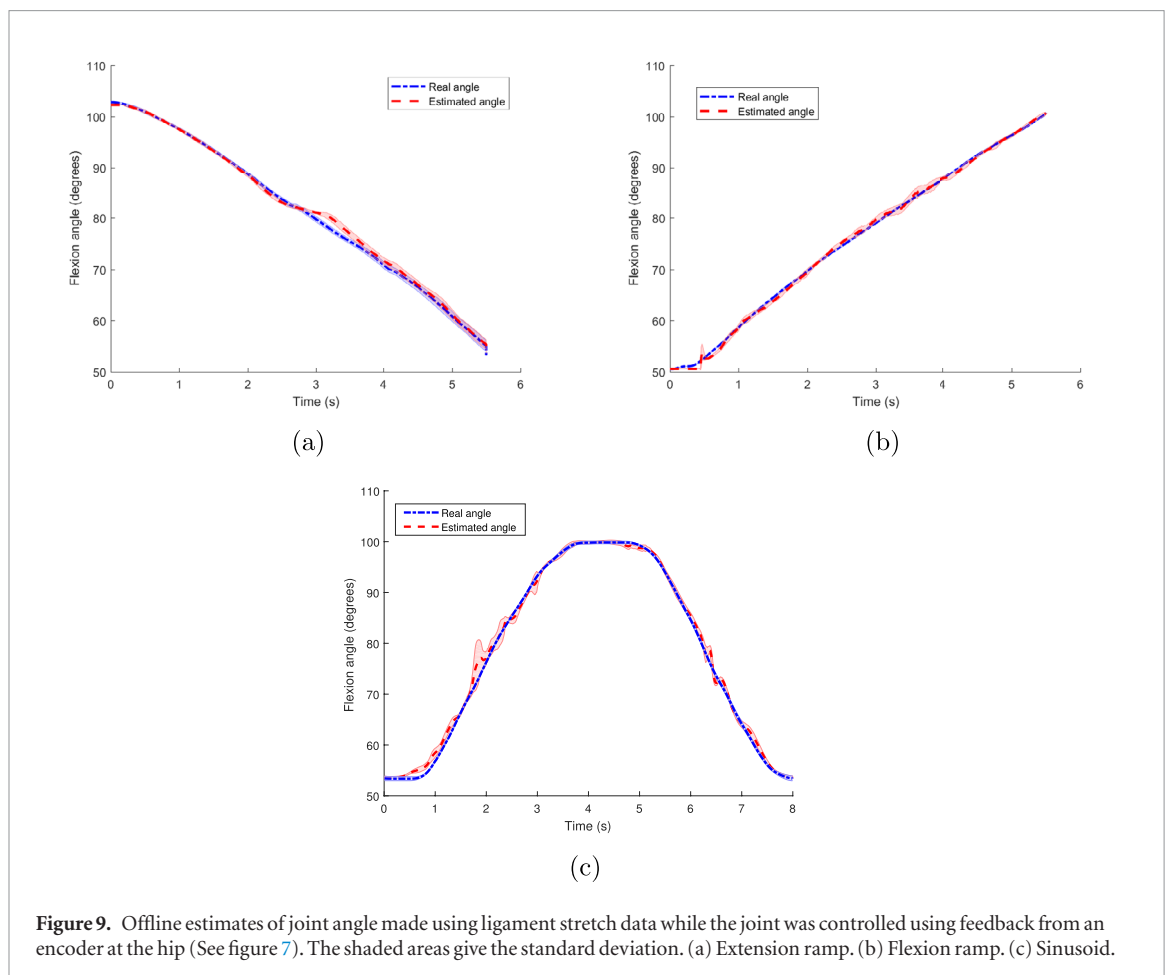


Figure 9. Offline estimates of joint angle made using ligament stretch data while the joint was controlled using feedback from an encoder at the hip (See figure 7). The shaded areas give the standard deviation. (a) Extension ramp. (b) Flexion ramp. (c) Sinusoid.

Table 3. Summary data for figure 9. Column 3 shows the mean squared error between the estimate of joint angle using the ligaments and the true joint angle ($degrees^2$). Column 4 gives the control error ($degrees^2$) for the joint when the encoder is used as the feedback to the PID controller. This last column can be compared to the control quality when the estimation using the ligaments is used as feedback to the controller. This is shown in table 4.

Test type	Figure	Integral of squared error between estimated and real joint angle	Integral of squared error between real joint angle and target angle
Extension ramp	9(a)	0.61 ($\sigma^2 = 2.50 \times 10^{-2}$)	1.88 ($\sigma^2 = 3.62 \times 10^{-2}$)
Flexion ramp	9(b)	0.49 ($\sigma^2 = 5.67 \times 10^{-2}$)	8.25 ($\sigma^2 = 9.37 \times 10^{-3}$)
Sinusoid	9(c)	1.61 ($\sigma^2 = 1.25$)	10.45 ($\sigma^2 = 2.02 \times 10^{-1}$)

to 51.8 mm at 43.9° found in humans [26]. This design also had the lowest maximum cable force, for stair ascent, per unit bodyweight of 22.5 N kg^{-1} . In both cases the biomimicking bicondylar joint, with a moving centre of rotation, allows a better fit to the human knee with a 30% and 20% reduction in absolute difference to the human knee moment arm, compared to a fixed centre of rotation, in the tibia and femur attached configurations, respectively.

For a sit-to-stand activity the maximum moment is required at the start of the process, when the flexion angle is close to 90° , dropping off towards 0° [41]. For gait the maximum moment is required when the flexion angle is 22° [7] and for stair ascent it is close to 60° [40]. This indicates that a large moment arm is most valuable in the mid range of joint motion, 20° – 90° of flexion. The smaller moment arm outside of this range reduces the stroke length required of the actuator moving the tendons. This happens because a small

moment arm requires a smaller amount of actuator movement for a given angle change. As a result, for stair ascent, it was possible to achieve a reduction in the required actuator volume of up to 12.1% compared to using a constant moment arm joint capable of lifting the same load. To put this in context, a 70 kg person would require an actuator with a peak force over 200 N smaller by using the bicondylar joint for extension. Novel designs such as Martinez-Villalpando's agonist-antagonist knee [6], which uses a linear actuator and constant radius hub, would be able to use a smaller motor for the same performance by replacing the hub at the joint with the bicondylar design. The weight of a currently available commercial powered lower leg prostheses is 33% heavier than the human shank (see section 1.1). By using smaller actuators, designs such as those presented here could have the potential to reduce

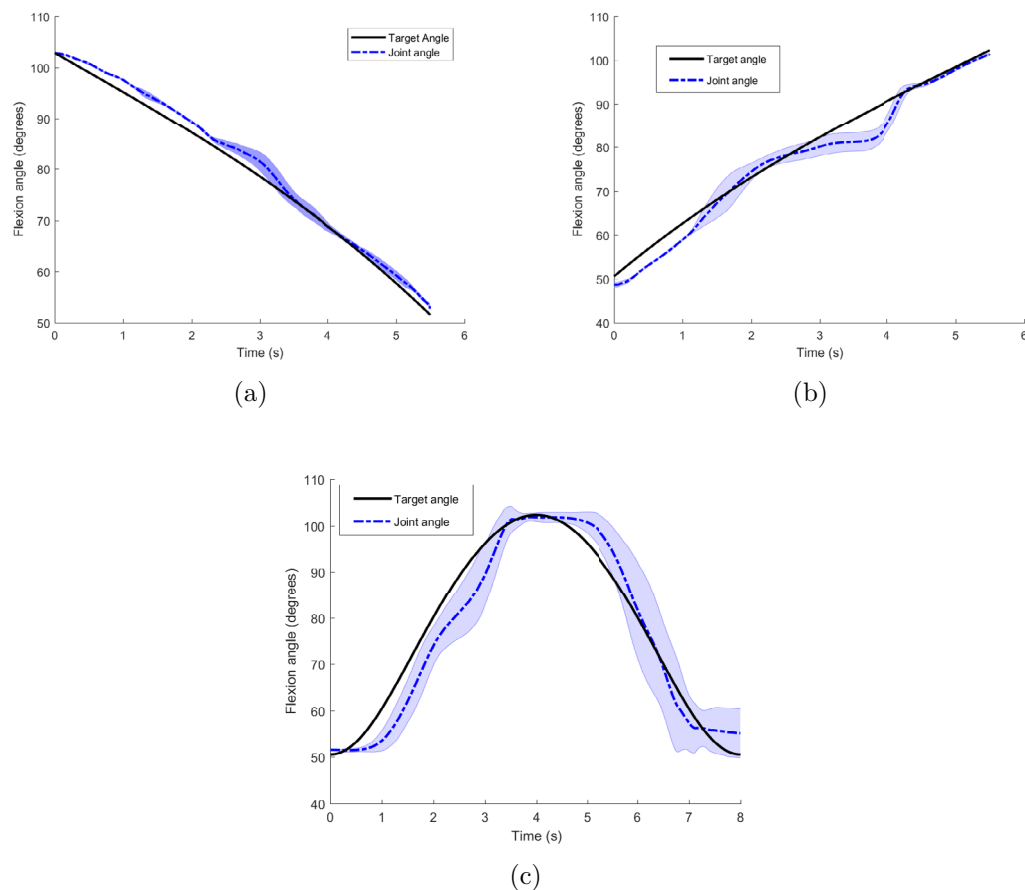


Figure 10. Control of joint angle using the mechanical ligament stretch data to estimate joint angle. The shaded area gives the standard deviation.

Table 4. Summary data for figure 10. Shown below is the control error when the angle estimate using ligaments lengths, processed with the neural net, is used as feedback to the PID controller. This can be compared to the error when the encoder is used as feedback given in column 4 of table 3.

Test type	Figure	Integral of squared error between real joint angle and target angle
Extension ramp	10(a)	2.57 ($\sigma^2 = 0.91$)
Flexion ramp	10(b)	11.39 ($\sigma^2 = 12.53$)
Sinusoid	10(c)	52.48 ($\sigma^2 = 3.05$)

this weight. At the same time, the gap in capability for high load tasks [16, 17] between intact and prosthetic limbs could be reduced.

A further benefit is that a moment arm that reduces close to maximum extension and flexion will reduce the magnitude of any moment attempting to hyperextend the joint. The ability of the joint to apply a moment reduces slowly towards the limits of its range rather than coming to a hard stop. As a result, a moment arm such as that shown in figure 8 will therefore exhibit improved safety for the same performance compared to a constant moment arm joint.

Using the same method described here it is possible to optimise the geometry, not for human moment arm matching, but for some other carefully selected objec-

tive. Future work will investigate whether improvements to joint performance can be obtained this way.

4.2. (ii) Ligament stretch for joint position estimation

This paper shows that ligament-like elastic elements in the joint can be used to estimate joint position (figure 9) and that these estimates can be used to control the joint (figure 10). There was, however, a reduction in controller performance with an increase of integral of squared error (ISE) of between 1.4 and 5 times for the extension and sinusoid tests respectively. The largest impact of using the ligament stretch for position control was upon the consistency of the response with a 10^3 change in the variance in the case of flexion ramp.

An additional limitation was that the neural net had to be trained on the same test type as that on which it was to estimate the joint angle i.e. the joint estimator for the flexion ramp test will only work when the joint is moving at an almost constant velocity in that one direction. It was also found that when the estimator was used as the feedback to the controller small fluctuations in the estimator were amplified by the control process which in turn induced larger than usual fluctuating forces in the system. The estimator was sensitive to these changing forces across the joint and its accuracy reduced. This explains why a controller using

this estimate was not able to follow the target path with a great deal of accuracy and, indeed, greater variance in control quality between individual tests was observed.

The sensitivity of the system to external forces on the joint is supported by previous work on the same first iteration of the joint [33]. Additionally, although there is evidence that ligament strain in humans and animals is used in control [25], studies have shown that deafferentation of ligament mechanoreceptors results in only a small loss in proprioception [42, 43]. This indicates that precise angle measurement using ligaments alone is unlikely.

However, the sensitivity of the ligament stretch measurements to external forces could well make it possible to use these measurements not for precise position estimation but, instead, for phase of gait and intent detection. The current state of the art is to perform this detection using IMU's or force sensors alongside a classifier [44, 45]. Ligament stretch from the bicondylar knee might provide a viable alternative. This will be an area for future research.

5. Conclusion

We have shown that it is possible to design a bicondylar joint with a similar moment arm profile to the human knee. This was done by adjusting only the patella and tendon attachment positions and without changing the geometry of the joint condyles themselves. The variable moment arm achieved here reduces the risk of hyperextension or sudden deceleration at the end of the joint range. At the same time the variable mechanical advantage produced means that the joint can be driven by linear actuators with a smaller volume than in a joint with a constant moment arm while achieving the same performance. One example application is to the agonist-antagonist knee from Martinez-Villalpando *et al* [6], which may see a reduction in motor mass by employing the biomimicking joint design.

Additionally, joint position estimation using the stretch in compliant ligaments has been performed in a bicondylar joint. This has been done successfully under tightly controlled conditions. The accuracy of the estimate was affected by both joint forces and the speed of movement and this negatively affected the quality of control that could be achieved.

The bicondylar joint described here has been designed with rolling, sliding, compliant and actuation mechanisms inspired by the human knee. The current results could be significant in the future design and control of robotic knees for exoskeletons, prostheses and walking robots. By incorporating the bicondylar joint into systems that are currently pin jointed, the minimum required actuator size can be reduced while still providing sufficient joint control thereby enabling a potential step-change in weight and efficiency for legged robotics.


Acknowledgment

Funding for this project was came from a UK EPSRC Doctoral Training Partnership (DTP) with Imperial College London. Additional funding has been provided by the City and Guilds College Association and the UK Medical Research Council (MRC) Council Confidence in Concept (CiC) Scheme.

ORCID iDs

Felix Russell  <https://orcid.org/0000-0003-2729-7847>

Yipeng Zhu  <https://orcid.org/0000-0003-3321-0832>

William Hey  <https://orcid.org/0000-0002-4371-3452>

Ravi Vaidyanathan  <https://orcid.org/0000-0002-9625-4544>

Peter Ellison  <https://orcid.org/0000-0003-3741-8219>

References

- [1] Seok S, Wang A, Chuah M Y, Otten D, Lang J and Kim S 2013 Design principles for highly efficient quadrupeds and implementation on the mit cheetah robot *IEEE Int. Conf. on Robotics and Automation* (IEEE) pp 3307–12
- [2] Bhounsule P A, Cortell J and Ruina A 2012 Design and control of ranger: an energy-efficient, dynamic walking robot *Proc. CLAWAR* pp 441–8
- [3] Torricelli D, Gonzalez J, Weckx M, Jiménez-Fabián R, Vanderborght B, Sartori M, Dosen S, Farina D, Lefeber D and Pons J L 2016 Human-like compliant locomotion: state of the art of robotic implementations *Bioinspir. Biomim.* **11** 051002
- [4] McGeer T 1990 Passive dynamic walking *Int. J. Robot. Res.* **9** 62–82
- [5] Pratt J E 2000 Exploiting inherent robustness and natural dynamics in the control of bipedal walking robots *Technical Report DTIC Document*
- [6] Martinez-Villalpando E C, Weber J, Elliott G and Herr H 2008 Design of an agonist-antagonist active knee prosthesis *2nd IEEE RAS and EMBS Int. Conf. on Biomedical Robotics and Biomechatronics* (IEEE) pp 529–34
- [7] Geeroms J, Flynn L, Jimenez-Fabian R, Vanderborght B and Lefeber D 2017 Design and energetic evaluation of a prosthetic knee joint actuator with a lockable parallel spring *Bioinspir. Biomim.* **12** 026002
- [8] Martinez-Villalpando E C, Mooney L, Elliott G and Herr H 2011 Antagonistic active knee prosthesis. a metabolic cost of walking comparison with a variable-damping prosthetic knee *Annual Int. Conf. of the IEEE Engineering in Medicine and Biology Society* (IEEE) pp 8519–22
- [9] Hamon A and Aoustin Y 2010 Cross four-bar linkage for the knees of a planar bipedal robot *10th IEEE-RAS Int. Conf. on Humanoid Robots (Humanoids)* (IEEE) pp 379–84
- [10] Greene M P 1983 Four bar linkage knee analysis *Orthot. Prosthet.* **37** 15–24
- [11] Hamner S R, Narayan V G and Donaldson K M 2013 Designing for scale: development of the remotion knee for global emerging markets *Ann. Biomed. Eng.* **41** 1851–9
- [12] Endolite 2015 Lower limb prosthetic product range *Catalogue 2015* (www.blatchford.co.uk)
- [13] Össur 2016 Össur Power Knee Technical Manual (www.ossur.co.uk)

- [14] De Leva P 1996 Adjustments to zatsiorsky-seluyanov's segment inertia parameters *J. Biomech.* **29** 1223–30
- [15] Highsmith M J, Kahle J T, Carey S L, Lura D J, Dubey R V and Quillen W S 2010 Kinetic differences using a power knee and c-leg while sitting down and standing up: a case report *J. Prosthet. Orthot.* **22** 237–43
- [16] Wolf E J, Everding V Q, Linberg A A, Czerniecki J M and Gambel C J M 2013 Comparison of the power knee and c-leg during step-up and sit-to-stand tasks *Gait Posture* **38** 397–402
- [17] Wolf E J, Everding V Q, Linberg A L, Schnall B L, Czerniecki J M and Gambel J M 2012 Assessment of transfemoral amputees using c-leg and power knee for ascending and descending inclines and steps *J. Rehabil. Res. Dev.* **49** 831
- [18] Girgis F G, Marshall J L and Jem A A M 1975 The cruciate ligaments of the knee joint: anatomical. Functional and experimental analysis *Clin. Orthopaedics Relat. Res.* **106** 216–31
- [19] Jones R, Nawana N, Pearcy M, Learmonth D, Bickerstaff D, Costi J and Paterson R 1995 Mechanical properties of the human anterior cruciate ligament *Clin. Biomech.* **10** 339–44
- [20] Smidt G L 1973 Biomechanical analysis of knee flexion and extension *J. Biomech.* **6** 79–92
- [21] Kurosawa H, Yamakoshi K-I, Yasuda K and Sasaki T 1991 Simultaneous measurement of changes in length of the cruciate ligaments during knee motion *Clin. Orthopaedics Relat. Res.* **265** 233–40
- [22] Hogervorst T and Brand R A 1998 Current concepts review-mechanoreceptors in joint function *J. Bone Joint Surg. Am.* **80** 1365–78
- [23] Ferrell W 1980 The adequacy of stretch receptors in the cat knee joint for signalling joint angle throughout a full range of movement *J. Physiol.* **299** 85
- [24] Kim A W, Rosen A M, Brander V A and Buchanan T S 1995 Selective muscle activation following electrical stimulation of the collateral ligaments of the human knee joint *Arch. Phys. Med. Rehabil.* **76** 750–7
- [25] Riemann B L and Lephart S M 2002 The sensorimotor system, part i: the physiologic basis of functional joint stability *J. Athletic Train.* **37** 71
- [26] Krevolin J L, Pandy M G and Pearce J C 2004 Moment arm of the patellar tendon in the human knee *J. Biomech.* **37** 785–8
- [27] Steele A G, Hunt A and Etoundi A C 2017 Development of a bio-inspired knee joint mechanism for a bipedal robot *Conference on Biomimetic and Biohybrid Systems* (New York: Springer) pp 418–27
- [28] Kikuchi T, Sakai K and Abe I 2016 Bioinspired knee joint for a power-assist suit *J. Robot.* **2016** 1
- [29] Asano Y, Mizoguchi H, Kozuki T, Motegi Y, Urata J, Nakanishi Y, Okada K and Inaba M 2013 Achievement of twist squat by musculoskeletal humanoid with screw-home mechanism *IEEE/RSJ Int. Conf. on Intelligent Robots and Systems* (IEEE) pp 4649–54
- [30] Pfeifer S, Riener R and Vallery H 2012 An actuated transfemoral prosthesis with optimized polycentric knee joint *4th IEEE RAS and EMBS Int. Conf. on Biomedical Robotics and Biomechatronics* (IEEE) pp 1807–12
- [31] Etoundi A, Burgess S C and Vaidyanathan R 2013 A bio-inspired condylar hinge for robotic limbs *ASME J. Mech. Robot.* **5** 1–8
- [32] Etoundi A C, Vaidyanathan R and Burgess S C 2011 A bio-inspired condylar hinge joint for mobile robots *IEEE/RSJ Int. Conf. on Intelligent Robots and Systems* (IEEE) pp 4042–7
- [33] Russell F, Gao L, Ellison P and Vaidyanathan R 2017 Challenges in using compliant ligaments for position estimation within robotic joints *IEEE Int. Conf. on Rehabilitation Robotics* (IEEE)
- [34] Perry J 1992 *Gait Analysis: Normal and Pathological Function* (Thorofare, NJ: Slack Books)
- [35] Isaza E, García L and Salazar E Determination of mechanic resistance of osseous element through finite element modeling *Proc. 2013 COMSOL Conf. (Boston)*
- [36] Fuss F K 1989 Anatomy of the cruciate ligaments and their function in extension and flexion of the human knee joint *American J. Anatomy* **184** 165–76
- [37] Cohen S B, VanBeek C, Starman J S, Armfield D, Irrgang J J and Fu F H 2009 Mri measurement of the 2 bundles of the normal anterior cruciate ligament *Orthopedics* **32** 687
- [38] Van Eijden T, De Boer W and Weijs W 1985 The orientation of the distal part of the quadriceps femoris muscle as a function of the knee flexion-extension angle *J. Biomech.* **18** 807–9
- [39] Haberland M and Kim S 2015 On extracting design principles from biology: I. Method—general answers to high-level design questions for bioinspired robots *Bioinspir. Biomim.* **10** 016010
- [40] Costigan P A, Deluzio K J and Wyss U P 2002 Knee and hip kinetics during normal stair climbing *Gait Posture* **16** 31–7
- [41] Yoshioka S, Nagano A, Hay D C and Fukushima S 2009 Biomechanical analysis of the relation between movement time and joint moment development during a sit-to-stand task *Biomed. Eng. Online* **8** 27
- [42] Ferrell W, Baxendale R, Carnachan C and Hart I 1985 The influence of joint afferent discharge on locomotion, proprioception and activity in conscious cats *Brain Res.* **347** 41–8
- [43] Folkow B *et al* 1969 The use of peripheral feedback in the control of movement *Science* **165** 911–3
- [44] Tucker M R, Olivier J, Pagel A, Bleuler H, Bourri M, Lamercy O, del R Millán J, Riener R, Vallery H and Gassert R 2015 Control strategies for active lower extremity prosthetics and orthotics: a review *J. Neuroeng. Rehabil.* **12** 1
- [45] Maqbool H F, Husman M A B, Awad M I, Abouhossein A, Iqbal N and Dehghani-Sanj A A 2017 A real-time gait event detection for lower limb prosthesis control and evaluation *IEEE Trans. Neural Syst. Rehabil. Eng.* **25** 1500–9